

RSC Advances



This is an *Accepted Manuscript*, which has been through the Royal Society of Chemistry peer review process and has been accepted for publication.

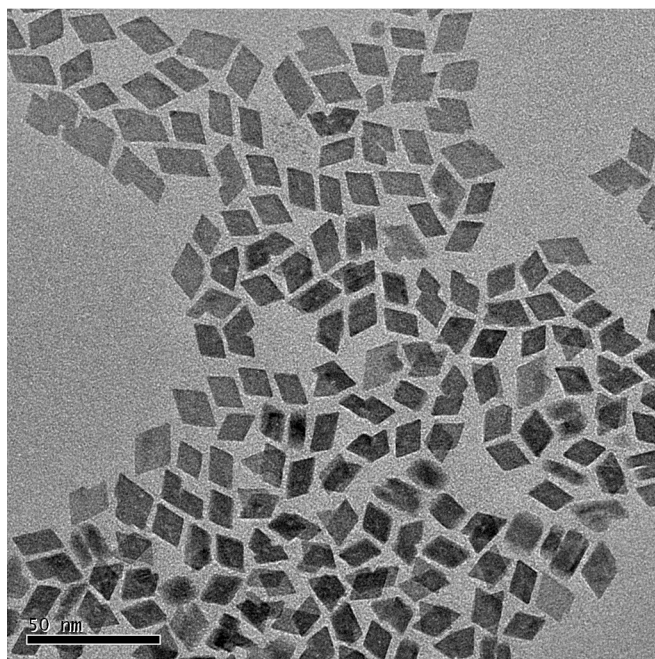
Accepted Manuscripts are published online shortly after acceptance, before technical editing, formatting and proof reading. Using this free service, authors can make their results available to the community, in citable form, before we publish the edited article. This *Accepted Manuscript* will be replaced by the edited, formatted and paginated article as soon as this is available.

You can find more information about *Accepted Manuscripts* in the [Information for Authors](#).

Please note that technical editing may introduce minor changes to the text and/or graphics, which may alter content. The journal's standard [Terms & Conditions](#) and the [Ethical guidelines](#) still apply. In no event shall the Royal Society of Chemistry be held responsible for any errors or omissions in this *Accepted Manuscript* or any consequences arising from the use of any information it contains.

Graphical Abstract

A novel monodisperse $\text{YbF}_3:\text{Er}^{3+}$ nanoplates with regular rhombus shape are synthesized via a thermolysis process in this study. The morphology and luminescence properties have been investigated using transmission electron microscopy (TEM) and emission spectroscopy.



COMMUNICATION

Synthesis of Monodispersed $\text{YbF}_3:\text{Er}^{3+}$ Nanoplates with Rhombus Shape

Cite this: DOI: 10.1039/x0xx00000x

Shengtai He,^{a*} Xiaoqin Hou,^a Jun Zhou,^a Yanan Li^a and Qing Li^a

Received 00th January 2012,
Accepted 00th January 2012

DOI: 10.1039/x0xx00000x

www.rsc.org/

A novel monodispersed $\text{YbF}_3:\text{Er}^{3+}$ nanoplates with rhombus shape are synthesized via a thermolysis process in this study. The morphology and luminescence properties have been investigated using transmission electron microscopy (TEM) and emission spectroscopy.

Controlling inorganic nanocrystals (NCs) with well-defined shapes and architectures is always an important route to finely tune their properties, because the properties of the materials closely interrelate with geometrical factors such as morphology, dimensionality, and size¹⁻³. In the past decade, lots of effort has been made to fabricate a variety of inorganic crystals to enhance their performance. Among them, the wet chemical method has been proved to be one of the most effective and convenient approaches in preparing various inorganic materials with diverse controllable morphologies and architectures in terms of low cost and large scale production.

In recent years, research on lanthanide (Ln^{3+}) ions doped fluoride crystals is rapidly increasing due to their wide applications in solar cell, flat panel display, fluorescence imaging, drug deliver⁴⁻⁸. The Ln^{3+} ions can undergo a process known as up-conversion (UC) in which they convert low energy radiation such as near infrared (NIR) or IR light to high energy radiation including visible or ultraviolet (UV) light^{9,10}. Typically in UC fluoride crystals, hexagonal (β) phase NaREF_4 (RE = rare earth ions) crystals are identified as the ideal UC luminescence matrices owing to their low phonon energy, high Ln^{3+} ion solubility and high photochemical stability¹¹⁻¹³. Besides β - NaREF_4 , orthorhombic REF_3 crystals have been proved to be another efficient high order UC luminescence materials¹⁴⁻¹⁶. Furthermore, $\text{YbF}_3:\text{Er}$ shows strong down-conversion properties when excited with UV light^{17,18}.

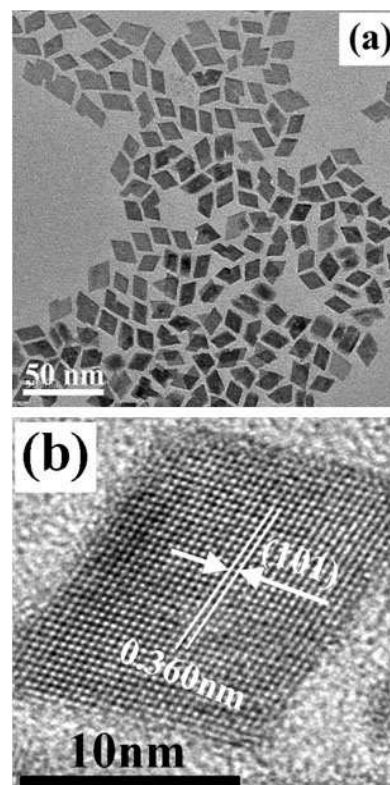


Fig.1 TEM (a) and HRTEM (b) images of as-synthesized $\text{YbF}_3:10\%\text{Er}^{3+}$ nanoplates.

Here, Er^{3+} doped YbF_3 rhombus nanoplates (NPs) are first synthesized with a high temperature thermolysis process. Fig.1a presents a TEM image of as-synthesized $\text{YbF}_3:10\%\text{Er}^{3+}$ NPs. It is found that almost all the nanoplate show clear rhombus shape and size of as-synthesized NPs is well dispersed. The length and width of NPs are 12.2 ± 2.1 nm and 10.9 ± 1.8 nm, respectively. The corresponding XRD and electron diffraction patterns (shown as S4 and S5) demonstrate that as-synthesized nanoplate is YbF_3

^a School of Materials Science and Engineering, Tianjin Polytechnic University, Tianjin 300387, China. E-mail: sh-t-he@tjpu.edu.cn; Tel: +86 (0)22 8395 5360; Fax: +86 (0)22 8395 5055.

† Electronic Supplementary Information (ESI) available: Detailed materials synthesis method and characterization data. See DOI: 10.1039/c000000x/

{Pnma} orthorhombic crystal structure. The diffraction band of as-synthesized nanoplates is consistent with the JCPDS 49-1805 file of crystal YbF_3 . Furthermore, from the high resolution TEM image of fig.1b, well crystalline lattice structures can be observed. Most of nanoplates grow along (101) with a lattice distance of 0.360 nm. The shape of YbF_3 nanoplate can be affected by the amount of Er^{3+} and oleic acid. Fig.2a presents a TEM image of YbF_3 : 50% Er^{3+} nanoplates. As shown in fig.2a, instead of well disperse single rhombus plate, short belts consisted by 2-4 single rhombus plates are observed for YbF_3 : 50% Er^{3+} plate. Fig.2b is a HRTEM image of an aligned YbF_3 :50% Er^{3+} plate standing on the edge array. The distance between two standing plate is about 2.5 nm, and the thickness of nanoplate is ca. 2.8 nm. The analysis results from HRTEM image of plate edge demonstrate that the edge grow along (111) and (020) directions. While, when amount of Er^{3+} is up to 90%, as-synthesized nanoplates are well disperse single rhombus plates (see S9). Furthermore, the shape or structure can be affected by the amount of oleic acid. For example, for YbF_3 :10% Er^{3+} discussed above, with same synthesis conditions, when volume of oleic acid is reduced from 3.2 ml to 1.6 ml, similar structure to that of YbF_3 : 50% Er^{3+} nanoplate are also observed. Currently, we attribute the formation of short belt of YbF_3 :10% to the overgrowth of nanoplate. With less oleic acid, several nanoplates grow and band together to form large nanoplate belt. Further experiments and analyses are being done to explore the effect of Er^{3+} amount and oleic acid on the structure of Er^{3+} doped YbF_3 nanoparticles.

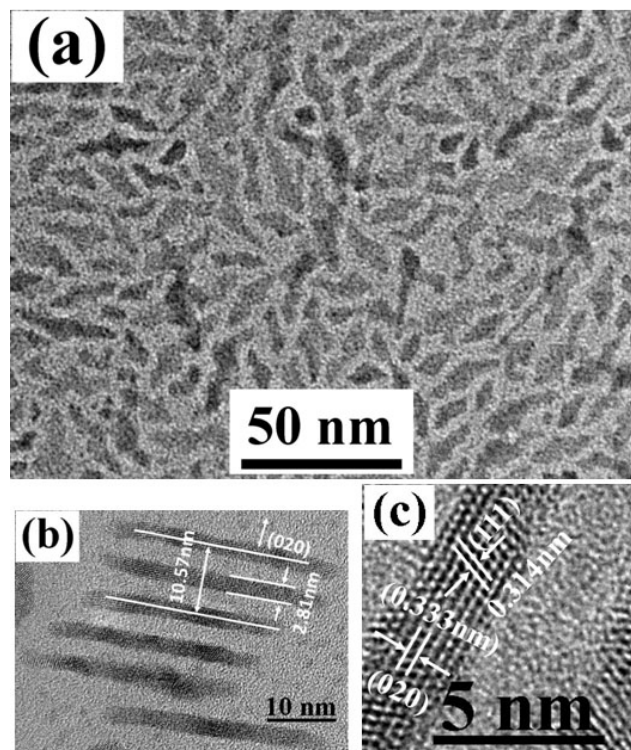


Fig.2 (a) TEM image of as-synthesized YbF_3 :50% Er^{3+} nanoplates, (b) HRTEM image of an aligned YbF_3 :50% Er^{3+} plate standing on the edge array. (c) HRETEM image of an aligned YbF_3 :50% Er^{3+} plate standing edge.

For the photovoltaic efficiency of semiconductor solar cells, the thermalization and sub-band gap losses with UV and near-infrared (NIR) are the major bottleneck. Up-conversion can generate one high energy photon from two or more incident low energy (sub-band gap) photons, whereas the down-conversion can generate more than one low-energy

(sub-band gap) photons for each incident high-energy photon. In this communication, we report the synergistic effect of UV down-conversion and NIR up-conversion of as-synthesized YbF_3 :10% Er^{3+} nanoplates.

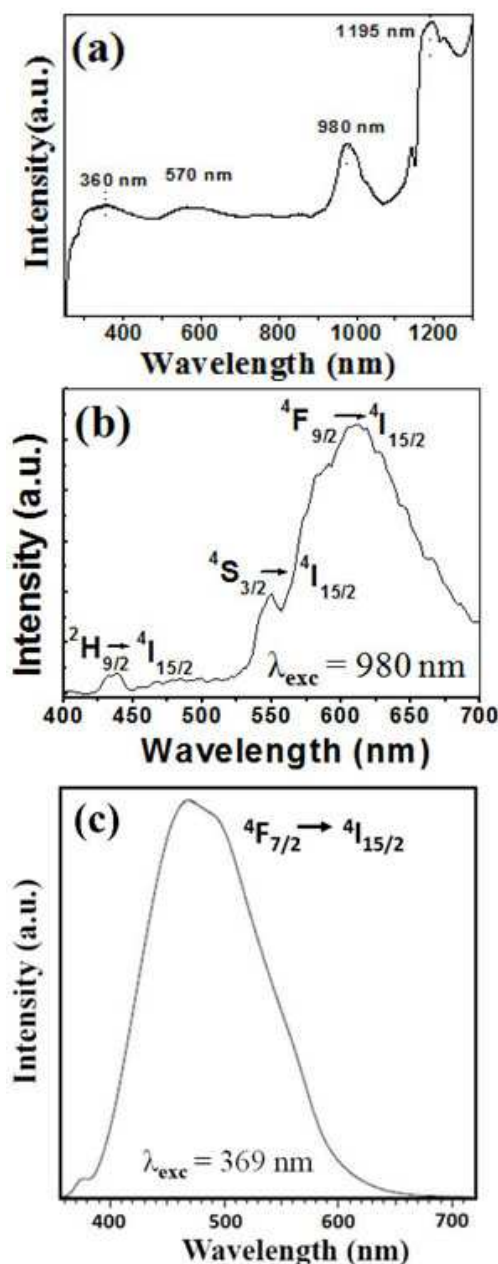


Fig.3 Absorption spectrum (a), upconversion (b) and downconversion (c) Emission of as-synthesized YbF_3 :10% Er^{3+} nanoplates (in b, the laser power of 980 nm laser diode is 1W.).

Fig.3 presents the absorption and emission spectra of as-synthesized YbF_3 :10% Er^{3+} NPs. It is well known that (Er^{3+} , Yb^{3+}) is one of the efficient up-conversion couples. Efficient up-conversion has been reported for this couple in many host lattices and it is used in the efficient detection of near 1000 nm IR radiation. After excitation to the $^2\text{F}_{5/2}$ level of Yb^{3+} , two sequential energy transfer steps excite the Er^{3+} ion from the $4\text{I}_{15/2}$ ground state to the $4\text{I}_{11/2}$ excited state and from the $4\text{I}_{11/2}$ excited state to the higher energy $4\text{F}_{7/2}$ excited state. Visible emission may be observed from the $4\text{F}_{7/2}$ state or, after relaxation, from the lower energy $2\text{H}_{11/2}$ and $4\text{S}_{3/2}$ states. Fig.3b is the UC emission spectra of as-synthesized YbF_3 :10% Er^{3+} NPs upon an excitation wavelength of 980 nm. The weak violet emission centred at 430

nm is attributed to the $^2H_{9/2} - ^4I_{15/2}$ transition of Er^{3+} ions. The obvious green emission peak at 542 nm is assigned to the $^4S_{3/2} - ^4I_{15/2}$ transition of the Er^{3+} ions, while the red emission peak at 610 nm is attributed to the $Er^{3+} \ ^4F_{9/2} - ^4I_{15/2}$ transition. Furthermore, (Er^{3+} , Yb^{3+}) couple is an attractive down-conversion (DC) materials for use in combination with c-Si solar cells¹⁹⁻²¹. The choice of Yb^{3+} as the emitting acceptor is due to the favourable energy of the $^2F_{5/2}$ excited state and the fact that the Yb^{3+} has no other 4f excited states that can interfere with the down-conversion process. Fig.3c shows a DC emission spectrum of as synthesized $YbF_3:10\% Er^{3+}$ NPs excited at 369 nm. The strong emission at 480 nm is attributed to the $^4F_{7/2} - ^4I_{15/2}$ transition of the Er^{3+} ions.

Conclusions

In this study, monodisperse Er^{3+} doped YbF_3 nanoplates with regular rhombus shape are synthesized by a thermolysis process. The as-synthesized $YbF_3:10\% Er^{3+}$ nanoplates are small and its size is less than 15 nm. The thickness of plate is about 2.8 nm. All the nanoplates are well dispersed and have a good crystalline. The analysis results demonstrate that the structure of plate can be affected by the amounts of doped Er^{3+} ion and oleic acid reagent. Moreover, the as-synthesized $YbF_3:10\%Er^{3+}$ nanoplates also show strong up-conversion and down-conversion emission properties.

This work is funded by National Key Basic Research Program (973 Program) of China (No. 2012CB933301) and Tianjin Research Program of Applied Basic & Cutting-edge Technologies (No. 09JCYBJC27200).

Notes and references

- 1 Y. Xia, Y. Xiong, B. Lim and S. Skrabalak, *Angew. Chem. Int. Ed.*, 2009, **49**, 60.
- 2 H. Chen, L. Shao, Q. Li and J. Wang, *Chem. Soc. Rev.*, 2013, **42**, 2679.
- 3 M. A. El-Sayed, *Acc. Chem. Res.*, 2001, **34**, 257.
- 4 J. W. Wang and P. A. Tanner, *J. Am. Chem. Soc.*, 2009, **132**, 947.
- 5 J. Bunzli, and S. V. Lanthanide, *J. Rare Earths*, 2010, **28**, 824.
- 6 M. Katkova, V. Ilichev, A. Konev, Irina I. Pestova, G. Fukin and M. Bochkarev, *Organic Electronics*, 2009, **10**, 623.
- 7 A. Yerpude and S. Dhoble, *Journal of Luminescence*, 2012, **132**, 1781.
- 8 F. Wang, Y. Han, C. Lim, Y. Lu, J. Wang, J. Xu, H. Chen, C. Zhang, M. Hong and X. Liu, *Nature*, 2010, **463**, 1061.
- 9 F. Auzel, *Chem Rev.*, 2003, 104, 139.
- 10 H. J. Wu, Z. W. Yang, J. Y. Liao, S. F. Lai, J. B. Qiu, Z. G. Song, Y. Yang, D. C. Zhou and Z. Y. Yin, *J. Alloys. Comp.*, 2014, **586**, 485.
- 11 Z. Wang, C.H. Liu, L.J. Chang and Z.P. Li, *J. Mater. Chem.*, 2012, **22**, 12186.
- 12 T. Jiang, Y. Liu, S.S. Liu, N. Liu and W.P. Qin, *J. Colloid Interface Sci.* 2012, **377**, 81.
- 13 Z. G. Yi, G. Z. Ren, L. Rao, H. B. Wang, H. B. Wang, H. R. Liu and S. J. Zeng, *J. Alloys Comp.* 2014, **589**, 502.
- 14 D.L. Gao, X.Y. Zhang, H.R. Zheng, W. Gao and E. J. He, *J. Alloys Comp.*, 2013, **554**, 395.
- 15 C.H. Liu, H. Wang, X. Li and D. Chen, *J. Mater. Chem.*, 2009, **19**, 3546.
- 16 G. S. Yi and G. M. Chow, *Adv. Funct. Mater.*, 2006, **16**, 2324.
- 17 X.F. Wang and X.H. Yan, *Opt. Lett.*, 2011, **36**, 4353.

- 18 Y. Zhang, R. Wang, S. Xiao, M. Qu, K. Li, C. Liu, X. Wang, X. Yan and H. Yan, *J. Luminescence*, 2014, **145**, 351.
- 19 P. Vergeer, T. J. H. Vlugt, M. H. F. Kox, M. I. Den Hertog, J. P. J. M. Van der Eerden, A. Meljering, *Phys. Rev. B*, **2005**, 71, 014119.
- 20 L. Aarts, B. M. van der Ende, A. Maljering, *J. Appl. Phys.*, **2009**, 106, 023522.
- 21 A. Wang, X. Yan, *Opt. Lett.*, **2011**, 36, 4353.